AIAA'84

AIAA-84-0397

Transient Temperature Rise of Arbitrary Contacts with Uniform Flux by Surface Element Methods

M.M. Yovanovich, K.J. Negus and J.C. Thompson, Univ. of Waterloo, Waterloo, Ontario, Canada

AIAA 22nd Aerospace Sciences Meeting

January 9-12, 1984/Reno, Nevada

TRANSIENT TEMPERATURE RISE OF ARBITRARY CONTACTS WITH UNIFORM FLUX BY SURFACE ELEMENT METHODS

M. M. Yovanovich*, K. J. Negus+ and J. C. Thompson+
Thermal Engineering Group
Department of Mechanical Engineering
University of Waterloo
Waterloo, Ontario, Canada

Abstract

An approximate but accurate solution has been obtained for the "long-time" temperature rise at the vertex of a right-triangle subjected to uniform flux during transient heat conduction into a semi-infinite solid. For "short-times" the temperature rise is determined from a sector of equal vertex angle and contact area. A criterion has been developed to determine the crossover from short to long time. Arbitrary contact shapes are discretized by combinations of these macro-surface elements to find the transient temperature rise at their common vertex. Excellent agreement is observed with the analytic solution for the circle, especially when the square root of the actual contact area is used to non-dimensionalize temperature and time. By means of an unique method of extrapolation, very accurate results are obtained for ellipses, rectangles and various other shapes over a wide range of dimensionless time.

Nomenclature

a	= radius of sector; semi-major axis of elliptical contact; half-width of rectangular contact
A_T	= total contact area
A_e	= error-causing area
b	= length of a side of a triangle; semi-minor axis of elliptical contact; half-width of rectangular contact
c	= length of a side of a triangle
Fo	= Fourier Modulus
Fo_{tr}	= transitional Fourier Modulus for "short-time" to "long-time" changeover
k	= thermal conductivity
ℓ	= chord length
N	= number of triangular elements
N_o	= initial number of equal-angle elements
q	= heat flux over contact
r	= polar coordinate
t	= time
T	= temperature rise
T_o	= centroidal temperature rise
T^*	= dimensionless temperature rise

Greek Symbols

α	= thermal diffusivity
δ	= length of perpendicular of a right-triangle
ε	= error in T^*
ρ	= polar coordinate
θ	= polar coordinate
ω	= vertex angle of a triangle or sector

Introduction

In many aerospace and industrial applications the temperature rise at a given point within a closed shape is required for a planar area with uniform flux. If a steady-state condition has been reached, then a surface element method developed by Yovanovich, Thompson and Negus[1] can be utilized. However, for planar areas subjected to uniform flux for some specified time, the problem becomes more complex.

One example of this type of problem is the thermal loading of microchips found in modern computers. These microchips, which can have thermal contacts of many different shapes, switch on and off continually at very short intervals. Another example is a machine tool contacting a work piece; in this case, there exists a rectangular thermal contact. Another example from the field of tribology, is a ball making contact with an inner or outer race; this creates an elliptical thermal contact. Also from tribology is the example of two rough surfaces moving relative to each other to produce elliptical contacts on a microscopic scale.

Unfortunately, even for relatively simple contacts such as ellipses and rectangles, solutions by analytical methods are extremely complex and solutions by numerical integration methods are very expensive.

The paper discusses the development and application of a right-triangular, transient, surface element to the determination of the transient temperature rise at arbitrary points located within arbitrary, planar contacts which are subjected to a uniform heat flux.

Short-time and long-time analytical expressions will be developed for the right-triangular, macro-element. A criterion will be given for the determination of short-time for the right-triangular element.

The paper discusses the unique method of employing the square root of the contact area to non-dimensionalize the temperature and time.

Temperature Rise at Vertex of a Right Triangle

For the problem illustrated in Fig. 1, the diffusion of heat from a point source qdA into a semi-infinite body or half-space with T=0 initially and an adiabatic surface, it has been shown that the incremental temperature rise T after some time t is given by [2]

$$T = \frac{q\,dA}{2\pi k\rho}\,\mathrm{erfc}\,(\rho/2\sqrt{\alpha t}) \qquad (1)$$

where k is the thermal conductivity of the body and α the thermal diffusivity.

If a uniform flux is precribed over a right-triangular contact area such as Fig. 2, the resulting temperature rise at the vertex is

$$T = \frac{q}{2\pi k}\int_0^{\omega}\int_0^{\delta/\cos\theta} \mathrm{erfc}\,(r/2\sqrt{\alpha t})\,dr\,d\theta \qquad (2)$$

Long-Time Solution

By assuming that t is 'large' then the argument of the complementary error function becomes

* Professor, Associate Fellow AIAA
+ Undergraduate Research Assistant
+ Associate Professor, Civil Engineering

small, or

$$\frac{r}{2\sqrt{\alpha t}} < 1 ,$$

and thus the complementary error function can be written as a series expansion [3] giving

$$T = \frac{q}{2\pi k} \int_0^{\omega} \int_0^{\delta/\cos\theta} \{1 - \frac{2}{\sqrt{\pi}} [\frac{r}{2\sqrt{\alpha t}} - \frac{r^3}{24(\alpha t)^{3/2}} + \frac{r^5}{320(\alpha t)^{5/2}} - \frac{r^7}{5576(\alpha t)^{7/2}} + \ldots]\} dr d\theta \qquad (3)$$

After evaluating these integrals[4] the temperature rise is

$$T = \frac{q}{2\pi k} \{\delta \ln(\tan (\frac{\pi}{4} + \frac{\omega}{2}) - \frac{\delta}{2\sqrt{\pi}\sqrt{Fo}} \tan \omega + \frac{\delta \sin\omega}{48\sqrt{\pi}\, Fo^{3/2}} [(\frac{2}{3} \sec\omega + \frac{1}{3} \sec^3\omega) - \frac{1}{20Fo} (\frac{8}{15} \sec\omega + \frac{4}{15} \sec^3\omega + \frac{1}{5} \sec^5\omega) + \frac{1}{448\, Fo^2} (\frac{16}{35} \sec\omega + \frac{8}{35} \sec^3\omega + \frac{6}{35} \sec^5\omega + \frac{1}{7} \sec^7\omega) - \ldots]\} \qquad (4)$$

where $Fo \equiv \alpha t/\delta^2$, The Fourier modulus or dimensionless time.

The first term of equation (4) is exactly the steady-state result of Yovanovich[5]. The additional terms represent a "correction" from the steady-state result. Note that the error associated with equation (4) increases with decreasing 'time' or Fo and with increasing angle ω because the series expansion of the complementary error function becomes invalid over some part of the

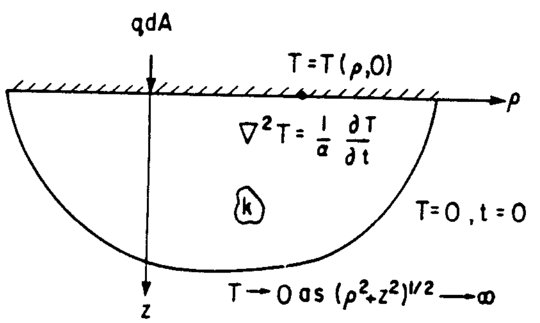

Fig. 1 Point source on adiabatic surface of a semi-infinite body

right-triangle's contact area.

Short-Time Solution

If it is assumed that the uniform flux over the right-triangular contact area has been applied only for a 'short' period of time, then it is reasonable to expect that the temperature rise at the vertex will be fairly insensitive to the details of the far boundary of the contact area. Thus for 'short' time only the temperature rise at the vertex of a right-triangle and a sector with the same vertex angle ω and contact area should be approximately identical. By equating the areas of the sector and right-triangle shown in Fig. 3 then

$$\frac{1}{2}\omega a^2 = \frac{1}{2}\delta^2 \tan\omega \qquad (5a)$$

or

$$a = \delta\sqrt{\frac{\tan\omega}{\omega}} \qquad (5b)$$

For the sector the temperature rise at the vertex is given by

$$T = \frac{q}{2\pi k} \int_0^{\omega} \int_0^{a} \operatorname{erfc}(r/2\sqrt{\alpha t})\, dr d\theta \qquad (6)$$

These integrations can be evaluated in closed form to give [2]

$$T = \frac{q}{2\pi k} \{2\sqrt{Fo'}\omega\, a[\frac{1}{\sqrt{\pi}} - \frac{1}{\sqrt{\pi}} \exp(-1/4Fo') + \frac{1}{2\sqrt{Fo'}} \operatorname{erfc}(1/2\, Fo')]\} \qquad (7)$$

where the Fourier modulus Fo' is now given by $Fo' \equiv \alpha t/a^2$.

The error associated with using equation (7) increases with increasing ω because the shapes of the sector and right-triangle become increasingly different. In addition the error also increases as Fo' increases since the shape differences noted above contribute more significantly to the temperature rise at the vertex.

Correlation Between Long-Time and Short-time Solutions

Equations (4) and (7) give respectively the temperature rise at the vertex of a right-triangle for the 'long'-time and 'short'-time assumptions. However, some criterion must be developed to determine for any particular angle ω the time t

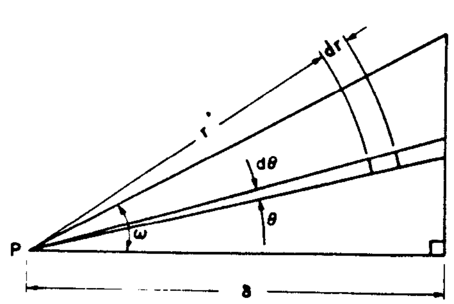

Fig. 2 Area integration of a right-triangle

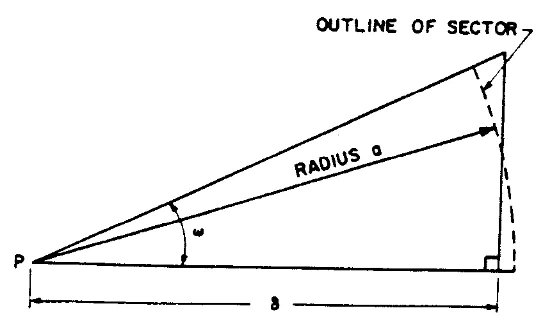

Fig. 3 Sector approximation of a right-triangle

which constitutes the transition from short-time to long-time. Since both equation (4) and (7) predict temperature rises slightly higher than those obtained by accurate numerical integration, then the transition time or transitional Fourier modulus Fo_{tr} for a particular ω occurs when the two solutions are identical. By investigating particular values of ω in 1-degree intervals from 0° to 85° the following correlations of Fo_{tr} as a function of ω have been made,

$$Fo_{tr} = \frac{1}{4\cos^2\omega}\{2.87 - 5.18\omega - 28.2\omega^2 + 95.6\omega^3 - \frac{2.31\times10^{-4}}{\omega}\}^2 \quad (8a)$$

for $0° < \omega < 15°$ $(0 < \omega \leq .2618$ rad.), or

$$Fo_{tr} = \frac{1}{4\cos^2\omega}\{.944 - .504\omega - .110\omega^2 + .119\omega^3 + \frac{.126}{\omega}\}^2 \quad (8b)$$

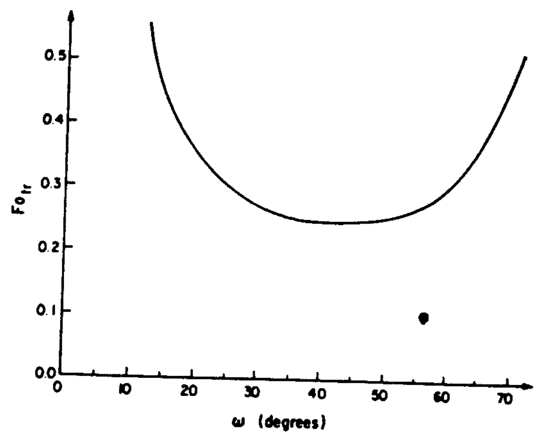

Fig. 4 Transitional Fourier modulus versus vertex angle

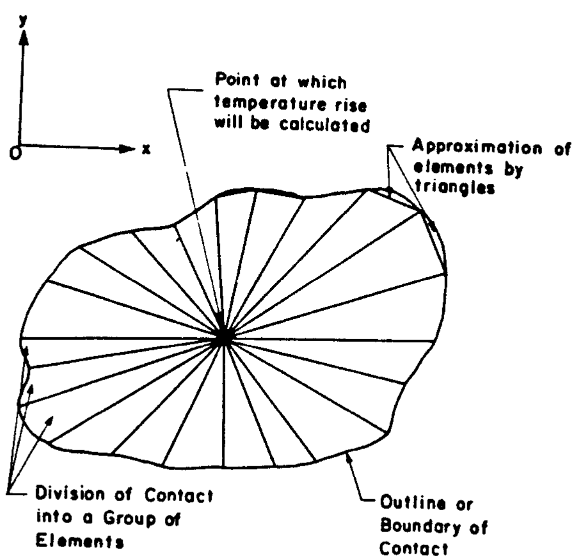

Fig. 5 Division of an arbitrary contact into triangular elements

for $15° < \omega < 85°$ $(.2618 < \omega < 1.4835$ rad) and in both (8a) and (8b) the angle ω is in radians and $Fo_{tr} \equiv \alpha t_{tr}/\delta^2$.

Fig. 4 shows the relationship between ω and Fo_{tr}. For vertex angles of less than 50° the maximum error, which occurs at Fo_{tr}, is about .5%. As the vertex angle ω approaches 75°, maximum error can reach 2-4%. However it must be noted that the actual error associated with some Fo falls very rapidly to zero as Fo goes above or below Fo_{tr}. In addition a technique will be discussed shortly which virtually eliminates all error for practical applications by making evaluations of the temperature rise by equation (4) or (7) with ω large and Fo close to Fo_{tr} unnecessary.

Application of Triangular Elements on Arbitrarily Shaped Contacts Division of Geometry into Elements

Any arbitrary contact geometry can be divided into elements starting from some internal point P at which the temperature rise is to be calculated. As shown in Fig. 5, each element is considered to

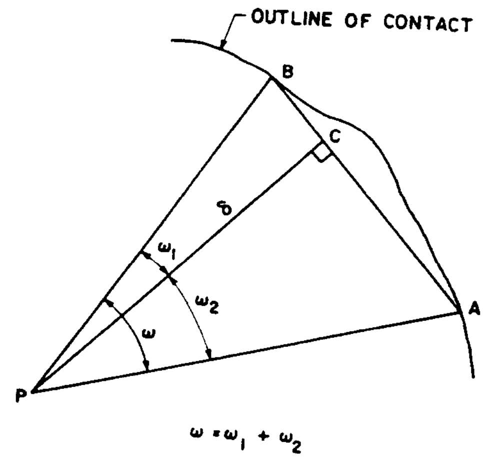

Fig. 6 Division of triangular element into two right-triangles: Case 1

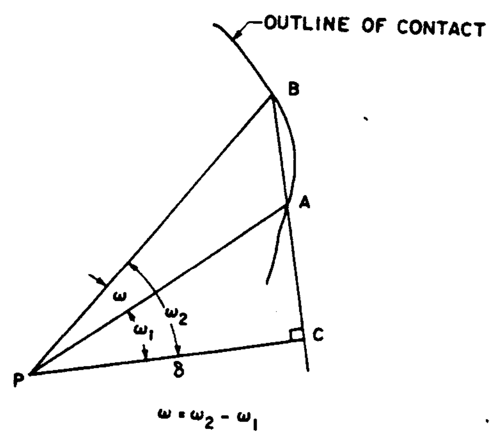

Fig. 7 Division of triangular element into two right-triangles: Case 2

be triangular in shape which implies that there will be some error in the final result since the actual shape is slightly different in area from that of the sum of the triangular elements.

Solution to a General Element

Any given triangular element can have one of the three orientations shown in Figs. 6, 7, and 8. Each orientation is just a linear combination of two right-triangles which will both have the same Fo.

If the temperature rise at the vertex of a triangular element with vertex angle ω is denoted by $T(\omega)$ then the following summary can be made:

Case 1. From Fig. 6,

$$T(\omega) = T(\omega_1) + T(\omega_2) \tag{9}$$

Case 2. From Fig. 7,

$$T(\omega) = T(\omega_2) - T(\omega_1) \tag{10}$$

Case 3. From Fig. 8,

$$T(\omega) = T(\omega_1) - T(\omega_2) \tag{11}$$

where $T(\omega_1)$ and $T(\omega_2)$ are determined by either equation (4) or (7) depending on the long-time or short-time criterion of equations (8a) and (8b).

Solution of Thin, Obtuse Triangular Element

In real applications of this method, thin, obtuse triangles as shown in Fig. 9 often arise. Since evaluation of the temperature rise at the vertex of this element involves two right-triangles which both have large vertex angles, substantial errors of 5-10% can arise when the Fourier modulus approaches Fo_{tr}. To overcome this problem a transformation is made from a thin, obtuse triangular element to a sector element of equal area. If the equal area sector has radius 'a' and the same vertex angle 'ω' then

$$\frac{1}{2}\omega a^2 = \frac{1}{2} bc \sin\omega \tag{12a}$$

or

$$a = \sqrt{\frac{bc \sin\omega}{\omega}} \tag{12b}$$

By recalling that equation (7) was derived for the temperature rise at the vertex of a sector this equation is valid again for this element giving,

$$T = \frac{q}{2\pi k} \{2\sqrt{Fo'} \quad \omega a \, [\frac{1}{\sqrt{\pi}} - \frac{1}{\sqrt{\pi}} \exp(-1/4Fo') + \frac{1}{2\sqrt{Fo'}} \operatorname{erfc}(1/2\sqrt{Fo'})]\} \tag{13}$$

where again $Fo' \equiv \alpha t/a^2$.

This method yields extremely accurate results when Fo approaches Fo_{tr} if the vertex angle ω is kept below 10 degrees. This requirement can always be met by further discretization of the contact shape when necessary. There are two reasons for the success of this technique. First, by keeping the vertex angle small, the differences in the far boundary shape between the sector element and the triangular element are minimal. Second, since this method is used when Fo is near Fo_{tr}, the dimensionless time is still relatively "short" so the minor differences in shape between the sector and triangular elements do not yet contribute significantly to the temperature rise at the vertex.

Within the actual computer program which was developed, the decision to use this sector approximation was based on several empirical criteria determined during the program development.

Method of Linear Extrapolation

After dividing a contact shape into N elements the total temperature rise at some internal point is simply,

$$T = \frac{q}{2\pi k} \sum_{i=1}^{N} T_i \tag{14}$$

A dimensionless temperature is now introduced by using the square root of the contact area as the fundamental length scale so that,

$$T^* = \frac{2\pi k T}{q\sqrt{A_T}} \tag{15}$$

where A_T represents the total area of the contact. Since the temperature rise is calculated from the

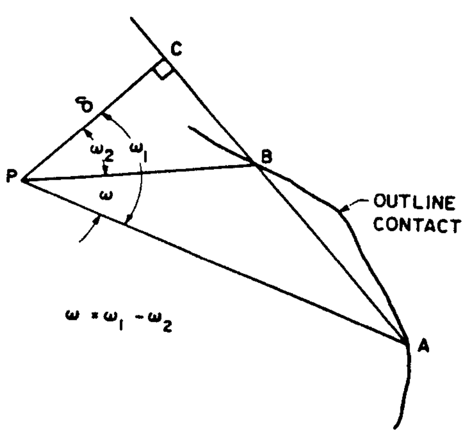

Fig. 8 Division of triangular element into two right-triangles: Case 3

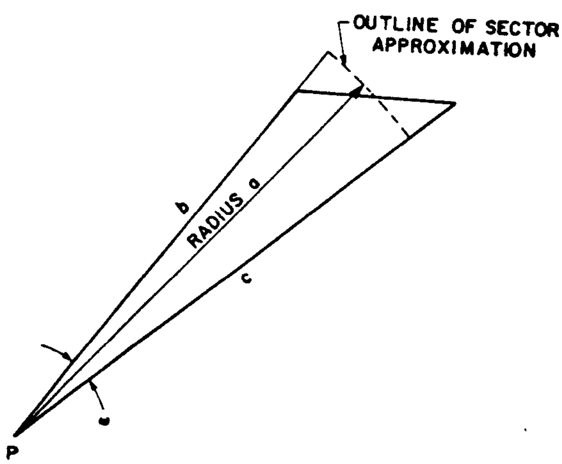

Fig. 9 Sector approximation of thin, obtuse triangular element

sum of triangular element temperature rises, then the total area A_T for non-dimensionalization should be the sum of the areas of the triangular elements

$$A_T = \sum_{i=1}^{N} A_i \tag{16}$$

where A_i is the area of the i^{th} triangular element.

However, since the actual continuous contact shape is approximated by triangles, the T* calculated will inherently be somewhat in error even if no errors occurred in the evaluation of each elemental contribution. This occurs because the T* calculated represents a shape with a slightly different boundary and area than the original contact. Thus error in T* arises from area differences lost or gained by the triangular elements.

Fig. 10 shows the location of the error-causing area A_e. From Fig. 10 it is also apparent that further division of the element will reduce A_e but will still keep A_e at about the same distance from P. Thus, if the error in T* is denoted by ε then,

$$\varepsilon \propto A_e \tag{17}$$

But if the boundary of the shape is considered circular locally then,

$$A_e \propto \ell^2 \tag{18}$$

where the chord length is related to the vertex angle ω such that,

$$\ell \propto \omega \tag{19}$$

If n equal-angle divisions of the contact shape are made to generate the elements then

$$\omega \propto 1/n \tag{20}$$

And therefore,

$$\varepsilon \propto 1/n^2 \tag{21}$$

Thus by plotting values of T* against $1/n^2$, where n is the number of equal-angle elements a linear relationship such as shown in Fig. 11 will be obtained. A simple extrapolation of this curve to the intercept where n = ∞ gives the T* of the actual contact shape. This technique has been used extensively with great success to generate the data of the next section and in every case a linear plot as shown in Fig. 11 has been observed.

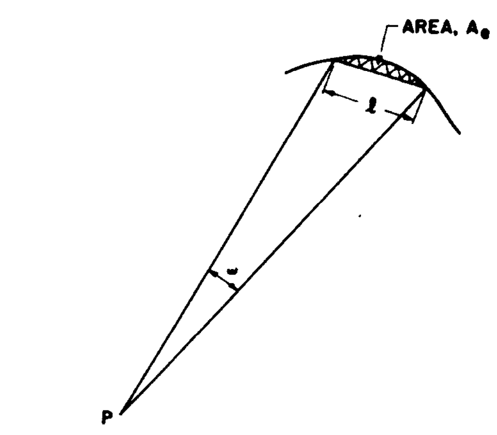

Fig. 10 Location of area unaccounted for by a triangular element

Results and Conclusions Regarding Dimensionless Temperature Rise at Centroid

Ellipses and Rectangles with Equal Aspect Ratio

To illustrate and apply the methods discussed, the dimensionless centroidal temperature rise has been calculated over a complete range of dimensionless time Fo where

$$T_o^* \equiv \frac{2\pi k T_o}{q\sqrt{A_T}} \tag{22}$$

and

$$Fo \equiv \frac{\alpha t}{(\sqrt{A_T})^2} \tag{23}$$

The ellipses are defined by $(x/a)^2 + (y/b)^2 = 1$ where the aspect ratio is b/a. The rectangles are of dimensions 2ax2b where again the aspect ratio is b/a. The resultant dimensionless centroidal temperature rises for ellipses and rectangles of different aspect ratios over the range of 10^{-6} to 10^6 for Fo are given in Tables 1 and 2 respectively.

The analytic solution for the circle is given by equation (7) by letting ω = 2π. This gives

$$T_o^* = 4\pi\sqrt{Fo}\,\Big[\frac{1}{\sqrt{\pi}} - \frac{1}{\sqrt{\pi}}\exp(-1/4\pi Fo) + \frac{1}{2\sqrt{\pi}\,\sqrt{Fo}}\,\mathrm{erfc}\,\Big(\frac{1}{2\sqrt{\pi}\,\sqrt{Fo}}\Big)\Big] \tag{24}$$

where $Fo \equiv \frac{\alpha t}{(\sqrt{A_T})^2} = \frac{\alpha t}{\pi a^2}$.

By evaluating this expression it can be shown that the results for the circle in Table 1 are all accurate to the decimal places shown. Note that for all these shapes symmetry was used so that calculations need only be made in the first quadrant. For the circle the necessary initial number of equal-angle elements was $N_o = 2$ (i.e. $2N_o = 4$, $4N_o = 8$). However, as the aspect ratio b/a decreased, the initial number of equal-angle elements increased to $N_o = 4$, $N_o = 8$ and

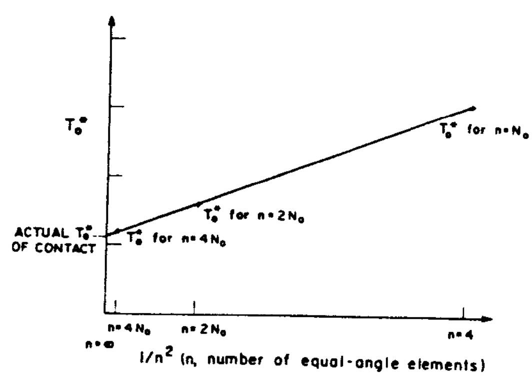

Fig. 11 Extrapolation of calculated temperature rises for a finite number of elements to the actual temperature rise of the contact

finally N_o = 16 for b/a = .1 in order to insure accuracy in every case to the decimal places shown. If less accuracy, say 1%, is all that is required then considerably fewer elements could be used.

From Tables 1 and 2 it is seen that the dimensionless centroidal temperature rise is always higher for the ellipse than the rectangle of same aspect ratio. However, by using the square root of area to non-dimensionalize the maximum difference observed is only about 4%. By inspection of Fig. 12 it can be seen that the shape difference between an ellipse and rectangle of the same aspect ratio shows up with the ellipse having more area concentrated near the centroid. This "extra" area which is concentrated near the centroid for the ellipse contributes more to the temperature rise than does the "lost" area at its far ends. Hence the ellipses have higher temperature rises, or alternatively an elliptical contact is more resistive than a rectangular contact with the same aspect ratio.

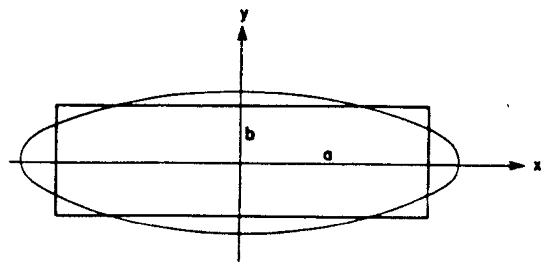

Fig. 12 Comparison of an ellipse and rectangle with equal area and aspect ratio

$Fo \equiv \frac{\alpha t}{(\sqrt{A_T})^2}$	Dimensionless Temperature, $T^* = \frac{2\pi k T_o}{q\sqrt{A_T}}$ at centroid of $(\frac{x}{a})^2 + (\frac{y}{b})^2 = 1$					
$\log_{10}$ Fo	b/a=1.0	b/a=0.8	b/a=0.6	b/a=0.4	b/a=0.2	b/a=0.1
-6	0.00709	0.00709	0.00709	0.00709	0.00709	0.00709
-5	0.02242	0.02242	0.02242	0.02242	0.02242	0.02242
-4	0.07090	0.07090	0.07090	0.07090	0.07090	0.07090
-3	0.2242	0.2242	0.2242	0.2242	0.2242	0.2242
-2	0.7090	0.7090	0.7089	0.7083	0.7001	0.6736
-1	1.9645	1.9574	1.9276	1.8493	1.6494	1.4113
0	2.9881	2.9773	2.9321	2.8137	2.4982	2.1070
1	3.3667	3.3558	3.3098	3.1894	2.8663	2.4601
2	3.4850	3.4775	3.4316	3.3110	2.9876	2.5809
3	3.5271	3.5161	3.4701	3.3496	3.0262	2.6195
4	3.5393	3.5283	3.4823	3.3618	3.0382	2.6317
5	3.5432	3.5322	3.4862	3.3656	3.0422	2.6355
6	3.5446	3.5334	3.4874	3.3669	3.0435	2.6368
∞	3.5449	3.5337	3.4878	3.3678	3.0442	2.6373

Table 1 Dimensionless centroidal temperature rise versus dimensionless time for ellipses

$Fo \equiv \frac{\alpha t}{(\sqrt{A_T})^2}$	Dimensionless Temperature, $T^* = \frac{2\pi k T_o}{q\sqrt{A_T}}$ at centroid of rectangles with dimensions 2a x 2b					
$\log_{10}$ Fo	b/a=1.0	b/a=0.8	b/a=0.6	b/a=0.4	b/a=0.2	b/a=0.1
-6	0.00709	0.00709	0.00709	0.00709	0.00709	0.00709
-5	0.02242	0.02242	0.02242	0.02242	0.02242	0.02242
-4	0.07090	0.07090	0.07090	0.07090	0.07090	0.07090
-3	0.2242	0.2242	0.2242	0.2242	0.2242	0.2242
-2	0.7090	0.7090	0.7089	0.7083	0.6938	0.6588
-1	1.9521	1.9430	1.9054	1.8108	1.5833	1.3559
0	2.9690	2.9560	2.9021	2.7639	2.4120	1.9990
1	3.3473	3.3341	3.2794	3.1389	2.7791	2.3505
2	3.4691	3.4459	3.4011	3.2606	2.9009	2.4713
3	3.5076	3.4944	3.4397	3.2906	2.9390	2.5098
4	3.5198	3.5066	3.4519	3.3114	2.9512	2.5220
5	3.5237	3.5105	3.4558	3.3152	2.9551	2.5259
6	3.5249	3.5117	3.4570	3.3164	2.9563	2.5271
∞	3.5255	3.5123	3.4575	3.3170	2.9569	2.5276

Table 2 Dimensionless centroidal temperature rise versus dimensionless time for rectangles

Comparison of Several Shapes

In Table 3 the dimensionless centroidal temperature rise of five different shapes are tabulated. From these results it is seen that the dimensionless centroidal temperature rise decreases as the contact shape becomes less concentrated about the centroid or with the semi-circle, less symmetric about the centroid.

In addition two major observations can be made from Tables 1, 2, and 3. First by using the square root of area to non-dimensionalize, the dimensionless centroidal temperature rise for most shapes up to a Fo of 10^{-2} (or up to a Fo of 10^{-3} for very thin shapes) is given simply by

$$T_o^* = \frac{2\pi k T_o}{q\sqrt{A_T}} = 4\sqrt{\pi}\ \sqrt{Fo} \qquad (25)$$

where $Fo = \frac{\alpha t}{(\sqrt{A_T})^2}$

And second, when the dimensionless time Fo reaches 10^2, the centroidal temperature rise of any shape is within about 2% of its steady-state value.

Summary

The transient temperature rise at an internal point in an arbitrary contact shape can be readily determined by discretization of the entire shape with triangular macro-surface elements. By using the long-time and short-time solutions presented in this work and non-dimensionalizing with respect to the square root of the actual contact area, very accurate results can be obtained from relatively few elements and little computational effort. For engineering accuracy even fewer elements are required.

When both time and temperature are non-dimensionalized by the square root of the actual contact area, all shapes exhibit an identical, dimensionless, transient, centroidal temperature response for very short dimensionless time. As dimensionless time increases, the dimensionless temperature rise at the centroid increases in a similar manner for all shapes with the greatest differences in temperature rise observed at the steady-state condition. Contact shapes which are both symmetric and concentrated about the centroid (e.g. circle or square) have the highest centroidal temperature rises, or alternatively, are the most resistive to heat flow.

Acknowledgements

The authors acknowledge the financial support of the National Sciences and Engineering Research Council of Canada under Grant No. A7455 to Dr. M. M. Yovanovich and Grant No. A7768 to Dr. J. C. Thompson.

References

[1] Yovanovich, M. M., Thompson, J. C., and Negus, K. J., "Thermal Resistance of Arbitrarily Shaped Contacts", Third International Conference on Numerical Methods in Thermal Problems, Seattle, Washington, Aug. 2-5, 1983.

[2] Carslaw, H. S., and Jaeger, J. C., Conduction of Heat in Solids, Oxford University Press, London, 1959.

[3] Abramowitz, M., and Stegun, I., Handbook of Mathematical Functions, Dover Publications, Inc., New York, 1971.

[4] Gradshteyn, I.S., and Ryzhik, I. M., Tables of Integrals, Series, and Products, Academic Press, New York, 1961.

[5] Yovanovich, M. M., "Thermal Constriction Resistance of Contacts on a Half-Space: Integral Formulation", AIAA Paper 75-708, AIAA 10th Thermophysics Conference, Denver, Colorado, May 27-29, 1975.

$Fo \equiv \frac{\alpha t}{(\sqrt{A_T})^2}$	Dimensionless Temperature, $T^* = \frac{2\pi k T_o}{q\sqrt{A_T}}$ at centroid of various shapes				
$\log_{10} Fo$	Circle	Square	Equilateral Triangle	$(\frac{x}{a})^{1/2} + (\frac{y}{b})^{1/2} = 1$, $\frac{b}{a} = 1$	Semi-circle
-6	0.00709	0.00709	0.00709	0.00709	0.00709
-5	0.02242	0.02242	0.02242	0.02242	0.02242
-4	0.07090	0.07090	0.07090	0.07090	0.07090
-3	0.2242	0.2242	0.2242	0.2242	0.2242
-2	0.7090	0.7090	0.7090	0.7090	0.7087
-1	1.9645	1.9521	1.9151	1.8989	1.8872
0	2.9881	2.9690	2.9111	2.8808	2.8731
1	3.3667	3.3473	3.2883	3.2571	3.2498
2	3.4850	3.4691	3.4100	3.3788	3.3715
3	3.5271	3.5076	3.4486	3.4174	3.4101
4	3.5393	3.5198	3.4608	3.4296	3.4223
5	3.5432	3.5237	3.4646	3.4335	3.4261
6	3.5446	3.5249	3.4659	3.4347	3.4273
∞	3.5449	3.5255	3.4664	3.4356	3.4281

Table 3 Dimensionless centroidal temperature rise versus dimensionless time for various shapes